

Review

A Short Review of Aerobic Oxidative Desulfurization of Liquid Fuels over Porous Materials

Bo Yuan ¹, Xiaolin Li ^{1,*} and Yinyong Sun ^{2,*}

¹ Institute of Intelligent Manufacturing Technology, Shenzhen Polytechnic, Shenzhen 518055, China; yuanbo@szpt.edu.cn

² MIT Key Laboratory of Critical Materials Technology for New Energy Conversion and Storage, School of Chemistry and Chemical Engineering, Harbin Institute of Technology, Harbin 150001, China

* Correspondence: lixiaolin0427@szpt.edu.cn (X.L.); yysun@hit.edu.cn (Y.S.); Tel.: +86-755-26731941 (X.L.)

Abstract: Oxidative desulfurization (ODS) has attracted much attention owing to the mild working conditions and effective removal of the aromatic sulfur-containing compounds which are difficult to desulfurize using the industrial hydrodesulfurization (HDS) technique. Molecular oxygen in ambient air have been recognized as an ideal oxidant in ODS due to its easy availability, non-toxicity and low cost in recent years. However, molecular oxygen activation under mild operating conditions is still a challenge. Porous materials and their composites have drawn increasing attention due to their advantages, such as high surface area and confined pore space, along with their stability. These merits contribute to the fast diffusion of oxygen molecules and the formation of more exposed active sites, which make them ideal catalysts for aerobic oxidation reactions. The confined space pore size offers a means of catalytic activity and durability improvement. This gives rise to copious attention toward the porous catalysts in AODS. In this review, the progress in the characteristics and AODS catalytic activities of porous catalysts is summarized. Then, emphasis on the molecular oxygen activation mechanism is traced. Finally, the breakthroughs and challenges of various categories of porous catalysts are concluded.



Citation: Yuan, B.; Li, X.; Sun, Y. A Short Review of Aerobic Oxidative Desulfurization of Liquid Fuels over Porous Materials. *Catalysts* **2022**, *12*, 129. <https://doi.org/10.3390/catal12020129>

Academic Editor: Haralampos N. Miras

Received: 25 November 2021

Accepted: 18 January 2022

Published: 21 January 2022

Publisher's Note: MDPI stays neutral with regard to jurisdictional claims in published maps and institutional affiliations.



Copyright: © 2022 by the authors. Licensee MDPI, Basel, Switzerland. This article is an open access article distributed under the terms and conditions of the Creative Commons Attribution (CC BY) license (<https://creativecommons.org/licenses/by/4.0/>).

Keywords: aerobic oxidation; oxidative desulfurization; porous materials; catalysis; liquid fuels

1. Introduction

Sulfur oxide (SO_x) emissions released from the combustion of residual sulfur compounds in liquid fuels causes severe environmental pollution, such as haze and acid rain [1]. To reduce pollution, numerous countries have issued a series of stringent regulations to limit the sulfur content in liquid fuels. Therefore, government departments all over the world issued a series of environmental protection regulations to limit the sulfur content in liquid fuels. In 2006, the US Environmental Protection Agency stipulated that the sulfur content in diesel fuel should not exceed 15 ppm, while the Euro V norms require that the sulfur content in liquid fuels is reduced to less than 10 ppm [2].

To meet the current sulfur content standards, many liquid fuels desulfurization technologies have been developed. Currently, the most adopted desulfurization method in industry is hydrodesulfurization (HDS) technology, which demands high temperatures and pressures (>630 K, >8 MPa), and large consumption of hydrogen. Furthermore, although HDS is effective for aliphatic organic sulfur compounds, mercaptans, thioethers and disulfides, it is ineffective for the removal of aromatic heterocyclic sulfur compounds in liquid fuels, especially large-molecular thiophene compounds, such as benzothiophene (BT), dibenzothiophene (DBT), 4,6-dimethyldibenzothiophene (4,6-DMDBT) and their alkyl derivatives [3,4].

To solve the above problems, non-HDS technologies have been developed, such as adsorptive desulfurization (ADS) [5–8], extractive desulfurization (EDS) [9–12], oxidative desulfurization (ODS) [13–15], and biodesulfurization (BDS) [16,17]. Among them, ODS

integrated with adsorption/extraction is receiving increasing attention, due to its non-hydrogen consumption, enhanced efficiency, mild reaction conditions, low cost, stronger operability, and practicability [18–21].

In the 1970s, some researchers began to use oxidizing gases containing nitrogen oxides to remove sulfides and nitrides contained in petroleum. Guth [22] first used nitrogen oxide as a chemical oxidant and methanol as an extractant to oxidize and remove sulfur and nitrogen compounds from petroleum. However, the ODS technology did not gain much importance until 2000, when stringent environmental regulations were declared. The oxidants commonly used in the oxidative desulfurization process are mainly NO_2 [23], organic peracids [24], hydrogen peroxide (H_2O_2) [25–28], organic hydrogen peroxide such as tert-butyl hydroperoxide (TBHP) and cumene hydroperoxide (CHP) [29–31], ozone [32–38], and air [39–41]. The oxidation capacity, reaction by-products, and prices of common oxidants in ODS reactions are shown in Table 1 [42]. From the perspective of environmental protection, hydrogen peroxide is considered to be a greener oxidant due to the by-product of the reaction being H_2O , and its oxidizing ability is high. The ODS mechanism regarding various oxidants have already been extensively discussed in previous review articles [42,43].

Table 1. Common oxidants and their oxidizing properties in ODS reactions of liquid fuels [42].

Oxidants	Active Oxygen (%)	Oxidizing Power (V vs. SHE)	Byproduct	Safety & Handling	Price (EUR/Kg)
H_2O_2 (30 wt%)	14.1(47.1)	+1.78	H_2O	Causes serious eye damage May cause respiratory irritation Causes skin irritation Keep from contact with clothing	145
Ozone	33.3	+2.07	SO_2	Very toxic to aquatic life Must be contained within ozone-resistant tubing and pipes	-
t-BuOOH(TBHP)	17.8	-	t-BuOH	Flammable liquid and vapor Causes severe skin burns and eye damage May cause genetic defects and cancer Use only under a chemical fume hood	64
CumOOH(CHP)	10.5	-	CumOH	Combustible liquid May be fatal if swallowed Avoid inhalation of vapor or mist	95
KO_2	45.0	+1.56	OH^-	May intensify fire; oxidizer Causes severe skin burns and eye damage Use only under a chemical fume hood	835
Organic peracid (peracetic acid at 100 wt%)	21.1	+1.81	Organic acid (acetic acid)	Flammable liquid and vapor Causes severe skin burns and eye damage; Avoid contact with skin and eyes	345
Air	23.2	+1.23 (O_2)	None	Contains gas under pressure, may explode if heated Store in a well-ventilated place	0

Basically, hydrogen peroxide is a 30% aqueous solution, which leads to a biphasic reaction system, increasing the mass transfer resistance between the oily and aqueous phase. Furthermore, the reaction system that uses H_2O_2 as the oxidant often requires the addition of a polar solvent or phase transfer agent to promote the mass transfer between different

phases. Most of the polar solvents are toxic, which undoubtedly increases the threats to environmental protection [44,45]. Alongside the environmental issues, the hydroperoxide also exhibit fire and explosion concerns [46]. An organic hydrogen peroxide, such as TBHP, CHP, etc. can be miscible with oil, so there is no need to add polar solvents or phase transfer agents to avoid the above problems. However, the organic alcohol's byproducts generated from organic hydrogen peroxide would be a contamination and affect the quality of liquid fuel products. Due to abundant sources, low cost and high environmental safety, air or oxygen have been increasingly used as an oxidant in oxidative desulfurization systems in recent years [47,48].

ODS with O_2 , also known as aerobic ODS (AODS), is gradually attracting interest. However, the activation of O_2 is still challenging under comparatively mild conditions since its ground state lies in triplet($3O_2$) with low energy [49,50]. Generally, this reaction has been carried out in pure O_2 at either high temperatures or elevated pressures, and it has usually required non-recyclable sacrificial agents. Therefore, the key issue in this field is to develop high-performance catalysts, aiming to reduce the requirement for O_2 activation [51,52]. As green chemistry and catalytic technology have been leaping forward, a noticeable progress has been achieved in the study on the AODS catalyst. Photocatalysis has shown a remarkable achievement in the activation of molecular oxygen [53–55]. A wide range of catalysts such as polyoxomolybdates [39], metal-organic framework materials [56,57], reduced graphene oxide (rGO) [58], boron nitride [59], precious metals [60], porphyrin [61], and metal oxides [62] have been reported.

Among them, the use of porous materials is highly desirable due to their large surface area and remarkable activity. The porous structure design is proposed to contribute to superior O_2 diffusion, more exposed active sites, tunable electronic structure, thus facilitating activation of O_2 . Furthermore, the confined space inside the pores could (i) create intimate contacts between the reactants and catalysts; (ii) offer particular microenvironment for the products formation; (iii) increase the power and energy densities of the pore confined fluids; (iv) make the surface active sites abundant; (v) accommodate and isolate active sites, enhancing stability and selectivity of exposed surface active centers; and (vi) facilitate the ion and electron transport, resulting in a tunable electronic structure and activation of molecular oxygen. The above confinement effects enable the thermodynamics and kinetics of the reaction be regulated, which eventually lead to catalytic performance enhancement.

Accordingly, the most recent available literature on development attempts for the commercially feasible and efficient porous materials AODS catalysts during the last decade is critically reviewed. In this review, the catalytic systems are first classified into porous metal oxides, molecular sieve and mesoporous silica, metal-organic frameworks, porous graphene, boron nitride-based materials, etc. Then, the structure and AODS performance developments of various porous catalysts made so far are summarized. The catalytic mechanism is also analyzed for each catalyst. Finally, based on a comparative analysis of the porous AODS catalysts, the limitations and prospects encountering in the development process are deliberated.

2. Porous Metal Oxides

Metal oxides have been used as catalysts for aerobic oxidative desulfurization extensively due to their low cost, facile synthesis, and superior catalytic performance [63,64]. Moreover, porous structure catalysts exhibit a higher catalytic activity since more active sites are exposed on their surface. On the other hand, the AODS process was classified as a gas-liquid-solid triple-phase reaction. The design of a hierarchical structure to enhance the mass transfer of O_2 from the gas-liquid interface to active sites undoubtedly played an important role in improving the apparent activity of catalyst. Therefore, porous metal oxides might be a promising candidate for the AODS process. In this section, porous metal oxides catalysts including molybdenum containing mixed metal oxides (MMOs), tungsten oxide, vanadium pentoxide was summarized in Table 2 and the AODS mechanism was analyzed.

Table 2. Comparison on the catalytic performance of porous metal oxides as AODS catalysts.

Catalyst	BET (m ² /g)	Catalyst Amount	Model Oil Volume	Model Solution	Sulfur (ppm)	Oxidant	Reaction Temperature	Reaction Time	Activity	Ref.
Ce-Mo-O	14	100 mg	20 g	Decalin	BT(500) DBT(500) 4,6-DMDBT(200)	O ₂	100 °C 100 °C 100 °C	360 min 480 min 480 min	97% 99% 99%	[62]
Co ₂ MoO	–	100 mg	20 g	Decahydronaphthalene	BT(500) DBT(500) 4,6-DMDBT(500)	Air	120 °C	360 min 180 min 180 min	88% 100% 100%	[65]
CoFeMo-MMO-2	73.62	20 mg	20 g	Diesel	BT(500) DBT(500) 4,6-DMDBT(500)	Air	100 °C	360 min 180 min 180 min	~92% 99.2% 99.2%	[66]
CoNiMo-HNT-2	114.7	20 mg	20 g	Decahydronaphthalene	BT (500) DBT (500) 4,6-DMDBT(500)	Air	110 °C 100 °C 110 °C	120 min 240 min 120 min	60% 100% 100%	[67]
3DOM WO _x -400	14.2	10 mg	20 mL	Dodecane	DBT(200) 4-MDBT(200) 4,6-DMDBT(200)	Air	120 °C 120 °C 120 °C	480 min 480 min 240 min	99% 99% 99%	[68]
α-V ₂ O ₅ nanosheets	-	10 mg	50 mL	Decahydronaphthalene	DBT(500) DBT(600) DBT(800) DBT(1000) 4-MDBT(500) 4,6-DMDBT(500)	Air	120 °C 120 °C 120 °C 120 °C 120 °C 120 °C	360 min 360 min 360 min 360 min 360 min 360 min	99.7% 98.7% 97.2% 95.5% 96.1% 92%	[69]
T-Nb ₂ O ₅	22.1	50 mg	20 mL	Dodecane	DBT(200) 4-MDBT(200) 4,6-DMDBT(200)	O ₂	130 °C	420 min	100% 100% 96%	[70]

Among them, molybdenum containing mixed metal oxides (MMOs), which possess advantages of cheap affordability, excellent stability, and a tunable electronic structure, are the most promising catalysts for aerobic application.

Shi et al. [62] synthesized a mesoporous Ce-Mo-O catalyst, which was proved to be highly active for aerobic oxidative desulfurization. The dibenzothiophene and 4,6-dimethyldibenzothiophene were almost completely converted without any additional sacrificial agent at 100 °C with O₂ bubbled in at ambient pressure, and the conversion of benzothiophene could reach 97%. It was assumed that oxygen was first activated by Ce species in the catalyst to form some reactive oxygen species. Subsequently, these oxygen species were further oxidized DBT into DBTO₂ with the assistance of Mo species in the catalyst.

Zhang et al. [65] prepared a Co-Mo-O bimetallic oxide catalyst. It could oxidize 92.2% DBT at 120 °C in a reaction time of 1 h and air flow of 30 mL/min. The high performance benefited from the synergistic effect of Co and Mo. The Co sites could first exhibit the activation of O₂ and then the active oxygen species further reacted with Mo sites before oxidation of sulfur-containing compounds.

Song et al. [66] synthesized durable Co-Fe-Mo layered mixed metallic oxides and realized complete conversion of DBT in 1.5 h at 120 °C with an air flow rate of 40 mL/min. The catalysts could be repeated eight times without an obvious decrease in reactivity. The authors reported that with the decrease of Mo content, the oxygen vacancies increased, thus the AODS performance was improved.

Liu et al. [67] fabricated hierarchical hollow Co-Ni-Mo-O mixed metallic-oxide nanotubes as catalysts in AODS. The catalyst achieved complete conversion of DBT and 4,6-DMDBT at 100 °C with an air flow rate of 25 mL/min. The improved AODS catalytic performance was attributed to the well-exposed metal centers, high concentrated oxygen vacancies and desired electronic structure, as shown in Figure 1.

Zhang et al. [68] successfully prepared a three-dimensional hierarchical porous tungsten oxide (3DOM) catalyst with rich oxygen defects for aerobic oxidative desulfurization of 4,6-dimethyldibenzothiophene. The unique hierarchical porous structure successfully eliminated the steric hindrance effect of 4,6-DMDBT. The as-prepared 3DOM WO_x-400 showed the aerobic oxidative desulfurization of over 99% in 4 h with an air flow of 100 mL/min, as depicted in Figure 2A. Moreover, sulfur removal remained at 99% after 5-time cycles, as

shown in Figure 2B, which would meet the requirement for industrial production of clean diesel. The abundant oxygen defects facilitated the activation of O_2 to $O_2^{\bullet-}$, which boosted the ODS efficiency.

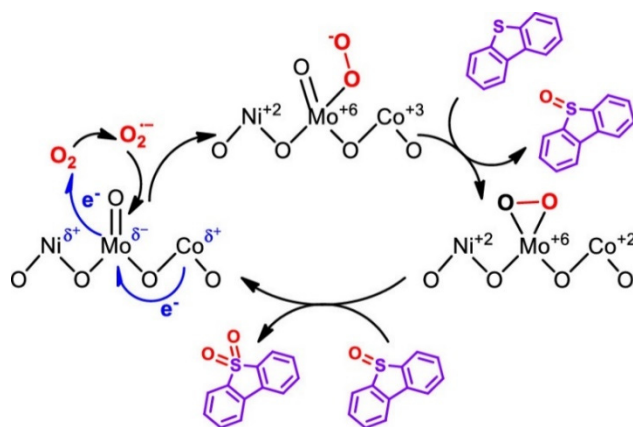


Figure 1. Proposed Catalytic Mechanism of Aerobic Oxidation of DBT Over CoNiMo Catalysts [67].

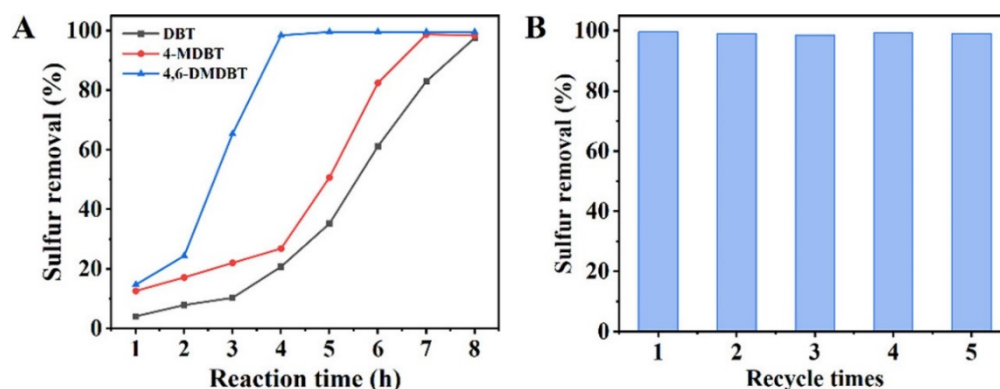


Figure 2. (A) Aerobic ODS tests on various sulfur compounds at 120 °C and (B) recycling performance of the 3DOM WO_x-400 sample [68].

Furthermore, orthorhombic vanadium pentoxide is always proposed to be advantageous for molecular oxygen (O_2) absorption and activation, thus it is a competent candidate in aerobic reactions.

Recently, Wang et al. [69] synthesized an atomic-layered α - V_2O_5 nanosheets (5–7 layers), resulting in a 99.7% sulfur removal of dibenzothiophene (less than 2 ppm) at 120 °C within 6 h and an air velocity of 100 mL/min. In this process, O_2 free from air is activated to $O_2^{\bullet-}$ by α - V_2O_5 nanosheets, which subsequently oxidize sulfur compounds to their corresponding sulfones, realizing deep desulfurization.

Yu et al. [70] synthesized an orthorhombic niobium pentoxide (T- Nb_2O_5) with elevated ratio of high-index planes, first for aerobic oxidative desulfurization (ODS) of the refractory aromatic sulfide. Compared with amorphous or pseudo-hexagonal mesoporous structure Nb_2O_5 , the 650 °C-T- Nb_2O_5 within 7 h had a 100% sulfur removal rate, showing its excellent catalytic performance. Moreover, the cycle experiments confirm the stability of the prepared 650 °C-T- Nb_2O_5 after 8 regeneration processes, showing a promising prospect of NbO_x-based materials for ODS under mild conditions.

3. Composites of Mesoporous Silica and Metal Oxides

Mixed oxides of transition metals are among the best studied catalysts for the oxidation of sulfur-containing compounds with atmospheric oxygen. However, fewer active sites are exposed in many bulk metal oxides due to the aggregation phenomenon. Thus, many carriers were developed to improve the dispersion of active species. The catalytic

performance comparison on composites of mesoporous silica and metal oxides was listed in Table 3.

Table 3. Comparison on the AODS catalytic performance of mesoporous silica/metal oxides composites.

Catalyst	BET (m ² /g)	Catalyst Amount	Model Oil Volume	Model Solution	Sulfur (ppm)	Oxidant	Reaction Temperature	Reaction Time	Activity	Ref.
5 wt%V ₂ O ₅ /SBA-15	547	50 mg	50 mL	Decahydronaphthalene	DBT (500)	Air	120 °C	480 min	99.3%	[71]
WO ₃ /MMS-500	167	10 mg	20 mL	Decalin	DBT (500) 4-MDBT(200) 4,6-DMDBT(200)	O ₂	120 °C	480 min	99.9% 98.2% 92.3%	[72]
CoMo-0.5IL-SBA	196	0.2 wt%	30 mL	Decalin	DBT (500) BT (500) 3-MBT (500)	Air	120 °C 120 °C 120 °C	90 min 180 min 360 min	100% 100% 57%	[73]
[(C ₈ H ₁₇) ₃ NCH ₃] ₃ -PMo ₁₂ O ₄₀ /γ-MMS	–	25 mg	20 mL	Decalin	DBT (500) 4-MDBT(500)	Air	120 °C	300 min 420 min	100% 100%	[74]

Wang et al. [71] reported a V₂O₅/SBA-15 composites synthesized by the impregnation methods. It was found that sulfur removal of DBT could reach 99.3% in the molecular oxygen-based system using ionic liquid extraction. Moreover, this reaction system was proved to be potential in practical application. The porous carrier (SBA-15) improved the dispersion of V₂O₅, which made more active sites exposed than bulk materials. The oxidative desulfurization efficiency for various organosulfur compounds was found in the following order: 4,6-DMDBT < 4-MDBT < DBT, as shown in Figure 3.

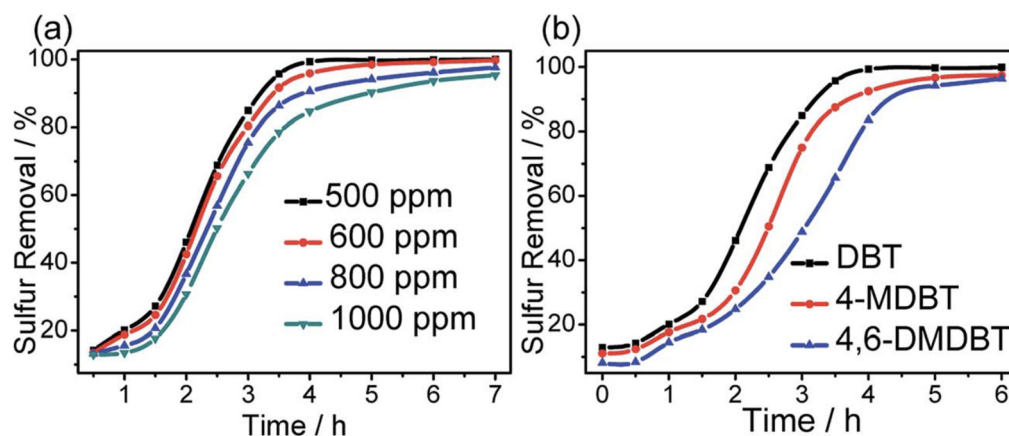


Figure 3. Sulfur removal of oils with different S-concentrations (a), and substrates (b). Experimental conditions: $T = 120\text{ }^{\circ}\text{C}$, $V(\text{oil}) = 50\text{ mL}$, $V(\text{Bmim}]\text{BF}_4) = 5\text{ mL}$, $m(\text{catalyst}) = 0.05\text{ g}$, $v(\text{air}) = 100\text{ mL min}^{-1}$ [71].

Jiang et al. [72] reported a novel tungsten oxide catalyst supported on magnetic mesoporous silica, where the removal of DBT could reach 99.9% after 8 h at 120 °C, as shown in Figure 4a. Moreover, the removal of 4-methyldibenzothiophene and 4,6-dimethyldibenzothiophene could also reach 98.2% and 92.3% under the same conditions, as shown in Figure 4b. FT-IR spectra indicated that tungsten peroxide formed during the reaction, thus the active species might be O₂^{•−} and tungsten peroxide.

For neat polyoxometalate (POM) and ionic liquid, the low surface area (<10 m²/g) and good solubility in polar solvents leads to the leaching of catalytically active sites. To overcome the limitations and improve the catalytic properties, the active components were immobilized on supports. Ekaterina A et al. [73] used an SBA-15 anchored Anderson-type POM as highly heterogeneous catalysts. A 100% DBT removal was achieved within 90 min at 120 °C at an air flow of 100 mL/min. By immobilization, the POM active center could be

reused five times without significant loss of catalytic activity, which overcame the drawback of neat POM catalysts.

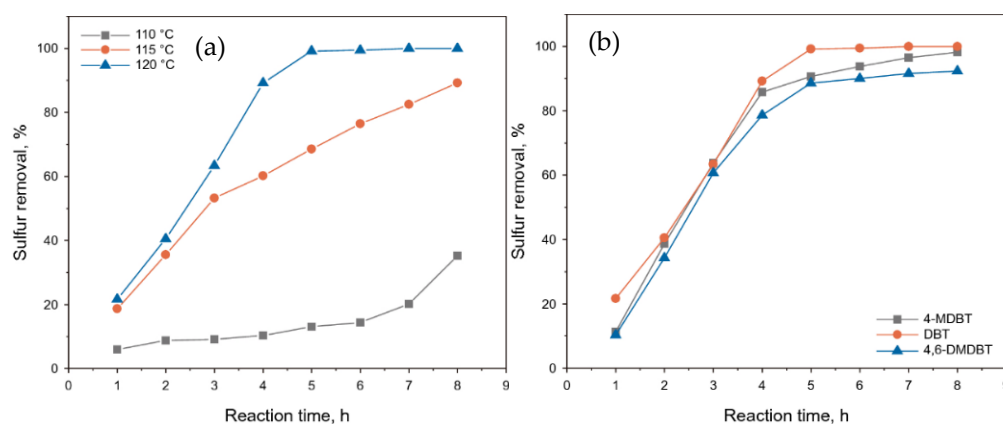


Figure 4. (a) Effects of different reaction temperatures on DBT removal. Reaction conditions: m (catalyst) = 0.01 g, air flow = 100 mL/min, and V (model oil) = 20 mL; (b) Removal of different substrates in the desulfurization system. Reaction conditions: m (catalyst) = 0.01 g, T = 120 °C, air flow = 100 mL/min, and V (model oil) = 20 mL [72].

Xun et al. [74] used magnetic mesoporous silica (γ -Fe₂O₃@Si@mSiO₂) as a support for an ionic liquid catalyst [(C₈H₁₇)₃NCH₃]₃PMo₁₂O₄₀. With air as an oxidant, the removal of DBT from model oil could reach 100% at 120 °C within 5 h and an air flow rate of 100 mL/min. Furthermore, the catalyst could be separated by a magnet and recycled at least four times without obvious decrease in the catalytic performance. It was suggested that Mo in [(C₈H₁₇)₃NCH₃]₃PMo₁₂O₄₀ could form active per-oxo groups and oxidize DBT to its corresponding sulfones.

4. Metal-Organic Frameworks Based Materials

Metal-Organic Frameworks (MOFs) are kinds of crystalline porous hybrid materials, which originate from the coordination bonds formed between metal nodes and organic linkers. Generally, MOFs have received increasing attention in various applications ranging from gas storage to chemical catalysis, owing to the excellent tunability of pore size, shape and functionality [75,76]. The combination of polynuclear metal clusters and organic linkers make them suitable catalysts for AODS. Furthermore, the high surface area makes MOFs affordable for accommodation of catalytic active species, thus forming MOF-supported catalysts. Their AODS catalytic performance is summarized in Table 4.

Table 4. Comparison on the AODS catalytic performance of MOFs-based materials.

Catalyst	BET (m ² /g)	Catalyst Amount	Model Oil Volume	Model Solution	Sulfur (ppm)	Oxidant	Reaction Temperature	Reaction Time	Activity	Ref.
POM@NENU-9N	564	44 mg	50 mL	Decalin	DBT(500)	O ₂	80 °C	90 min	100%	[77]
MIL-101 (Cr)	1850	0.5 g /L	10 mL	n-dodecane	DBT (200)	O ₂	120 °C	1440 min	99%	[56]
MIL-101 (Cr)-NO ₂	1850	0.04 mmol Cr	20 mL	n-dodecane	DBT (200)	O ₂	140 °C	270 min	100%	[78]
MFM-300(V)	993	1.5 g/L	5 g	n-dodecane	BT(200) DBT(200) 4,6-DMDBT(200)	ambient air	120 °C	300 min	12% 99.6% 98.1%	[57]
HPW@MOFs	1102	4.21 mg	60 mL	Octane	DBT(500)	O ₂	90 °C	240 min	84%	[79]
POM@MOF-199@MCM-41	732	2 g /L	-	Octane	DBT (2000)	O ₂	85 °C	180 min	98.5%	[80]
CNTs@MOF-199-Mo ₁₆ V ₂	371.45	100 mg	50 mL	n-octane	DBT (2000)	O ₂	80 °C	180 min	98.3%	[81]

For example, a MOF (NENU-9N) encased POM catalyst [77] was proved to be able to realize complete aerobic oxidative desulfurization of DBT at 80 °C for 1.5 h under the existence of isobutylaldehyde, which was first oxidized to the corresponding peracid by molecular oxygen and then oxidized DBT to DBT-sulfone. The nanocrystalline MOF facilitated POMs to overcome the obstacle of poor solubility in non-polar environment. However, the use of sacrificial agents increases the contamination of liquid fuel products.

Gómez-Paricio et al. [56] reported the desulfurization of DBT and its derivatives using MIL-101 as catalysts and molecular oxygen as oxidant without the need for sacrificial aldehydes. The reaction took an induction period of 6 h resulting from the diffusion of the solvent inside the MIL-101 pores. The authors envisioned that the shorter chain length of the solvent, the shorter the induction duration. The DBT could be completely oxidized into DBT-sulfone at 120 °C and 24 h, with an oxygen balloon under 1 atm. The resulting model oil extracted with water realized the complete removal of sulfur. In addition, the catalyst remains stable after five cycles without any activity reduction, showing a high stability. Selective quenching experiments confirmed $O_2^{\bullet-}/HOO^{\bullet}$ was the reactive oxygen species in the AODS reaction. About 1% solvent oxidation byproducts was observed.

On this basis, Vallés-García et al. [78] studied a series of MIL-101(Cr)-X functionalized with electron withdrawing (NO_2 , SO_3H or Cl) or electron donor (NH_2 or CH_3) groups, and found that the NO_2 -modified MIL-101 was more efficient than the parent MIL-101(Cr), and other isorecticular solid in promoting the AODS of DBT without any byproduct formation. The initial reaction rate was in a good linear relationship with the oxidation potential of the substituents on terephthalate ligands, thus MIL-101(Cr)- NO_2 was the most active catalyst. Mechanistic studies showed that MIL-101(Cr)- NO_2 was acting as heterogeneous catalyst in thiophenol oxidation and as a radical initiator for the AODS, as shown in Figure 5. For both reactions, the catalyst can be reused without deactivation, keeping its crystallinity and with negligible metal leaching.

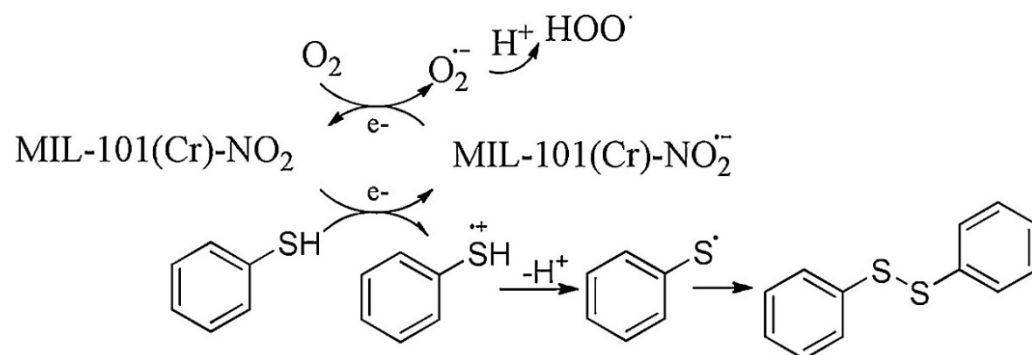


Figure 5. Proposed pathway for the aerobic oxidation of thiophenol to benzene disulphide using MIL-101(Cr)- NO_2 as catalyst [78].

Li et al. [57] investigated the AODS performance of MFM-300(V) in both hydrogen-donating and withdrawing solvents under ambient air atmosphere. The removal of sulfur content in model oil reached 99.6% and 98.1% for DBT and 4,6-DMDBT, respectively, in absence of molecular oxygen pumped or bubbled from the gas cylinders. The catalyst could be recycled seven times without any significant decrease in aerobic desulfurization performance. Moreover, the MFM-300(V) also showed excellent performance in both hydrogen-donating and hydrogen-withdrawing solvent. As depicted in Figure 6, the excellent AODS performance might be attributed to the active V-sites and unique porous structure of MFM-300(V), consequently facilitating the in-situ generation of $^{\bullet}OH$ radicals.

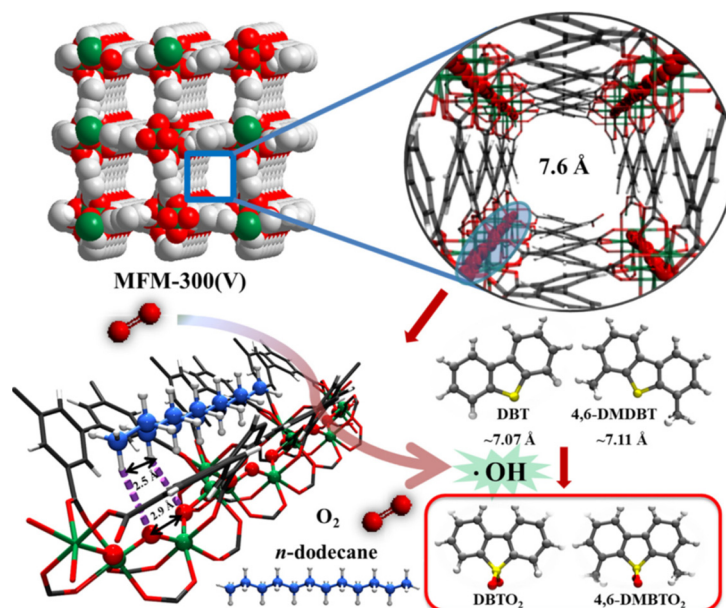


Figure 6. Proposed reaction mechanism over MFM-300(V) in ODS of DBT under ambient air atmosphere [57].

Ding et al. [79] first selected phosphotungstic acid in a host matrix (HPW@MOFs) as a recyclable and efficient catalyst in the AODS process. The effect of varying the flowrate of molecular oxygen was investigated for variance between 0 mL/min to 130 mL/min. The DBT conversion increased by increasing the flowrate of molecular oxygen and exhibited the best ODS performance at 110 mL/min, as shown in Figure 7. The mechanism of decreased ODS performance at high flowrate was attributed to the shortened contact between DBT and oxygen. In addition, the effect of increasing catalyst dosage was also reported in this work. The DBT conversion was significantly increased by increasing the HPW@MOFs dosage from 0% to 3% and 84% of DBT was removed from the model oil after 240 min.

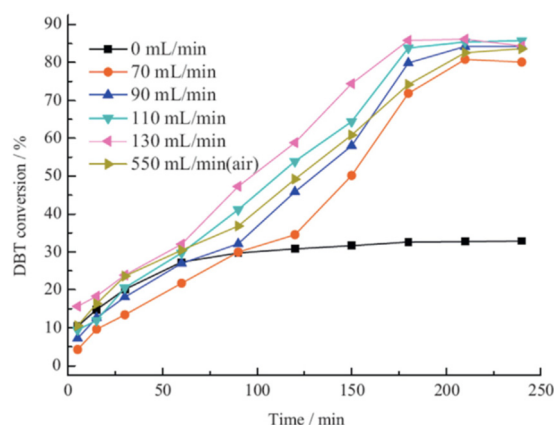


Figure 7. Effect of air and O₂ flow rate on DBT removal rate with HPW@MOFs. Conditions: reaction temperature, 90 °C; catalyst dosage, 1% the mass of normal octane; extracting agent, distilled water; reaction time, 240 min [79].

A catalyst system of POM@MOF-199@MCM-41(PMM) was designed by Li et al. [80] designed for deep oxidative desulfurization of model oil under O₂ atmosphere. The PMM catalyst showed a clearly nano-porous structure and definitely higher reactivity and stability compared with the heteropolyacid only. The DBT conversion could reach up to 98.5% when reacted for 3 h at 85 °C. Moreover, the catalyst could also be recycled and

reused for up to 10 cycles with minimal efficiency reduction, as shown in Figure 8. The pseudo-first-order reaction kinetics was followed.

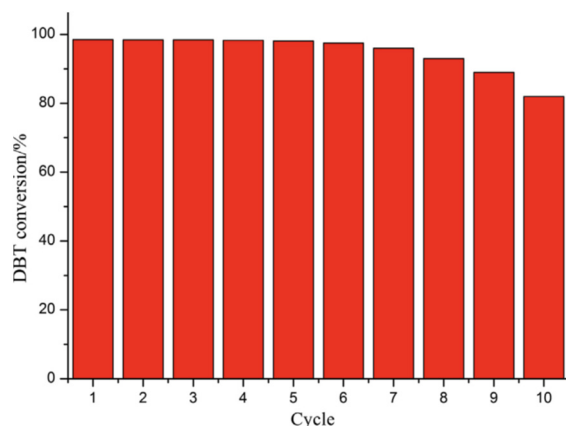


Figure 8. Stability test results of the catalyst [80].

Gao et al. [81] synthesized a series of CNTs@MOF-199-POM catalysts and tested for the oxidative desulfurization performance. Of all as-prepared catalysts, the CNTs@MOF-199-Mo₁₆V₂ catalyst showed the best catalytic results ranging up to 98.3% with an oxygen flow rate of 1.5 L/min at 80 °C in 180 min. The catalyst is valid from 40 °C to 100 °C, and the apparent activation energy calculated from pseudo-first-order rate constant is 12.89 kJ/mol, as illustrated in Figure 9. It was observed that the increase in agitation rate from 200 to 800 rpm led to significantly improving in oxidative desulfurization performance from 70% to 97%. Moreover, the as-prepared catalyst was tested for reusability and found to be usable for up to seven cycles. It was reported that M(O)_n– (M = Mo or V) in POM could combine with the oxygen to form M(O₂)_n– and then oxidize DBT into DBT-sulfone.

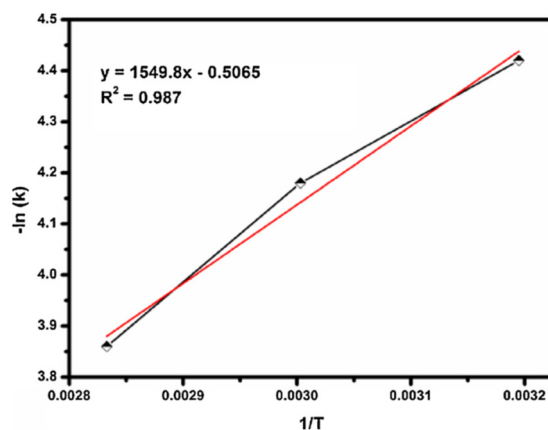


Figure 9. Plot of the inverse of temperature (1/T) versus root of the reaction rate constant $-\ln(k)$ [81].

5. Porous Graphene and Boron-Nitride Based Materials

Graphene-based materials have emerged as promising alternatives or supports to conventional metal-based catalysts, owing to their outstanding physicochemical characteristics, including high surface area, rich surface defects or functional groups, excellent mechanical stability, etc. [82–84]. Such merits integrated with low cost, non-toxicity and large-scale productivity made graphene-based materials competitive candidates for aerobic oxidation reactions [85]. On the other hand, another 2D materials, boron nitride, also known as “white graphite”, are recognized as an analogy to graphene. Therefore, recently boron nitride-based materials, such as hexagonal boron nitride (h-BN), graphene-like boron nitride (g-BN), and hexagonal boron carbon nitride (h-BCN) have been used as low cost

with excellent aerobic ODS performance in liquid fuels [86,87] The AODS performance for porous graphene and boron-nitride-based materials were summarized in Table 5.

Table 5. Comparison on the catalytic AODS performance for porous graphene and boron-nitride-based materials.

Catalyst	BET (m ² /g)	Catalyst Amount	Model Oil Volume	Model Solution	Sulfur (ppm)	Oxidant	Reaction Temperature	Reaction Time	Activity	Ref.
rGO	492	5 mg	25 mL	Dodecane	DBT(400) BT(400) 3-MBT(400) 4,6-DMDBT(400)	O ₂	140 °C	360 min	100% 90.5% 96.1% 97.7%	[58]
POM/PIL/Gr	83.4	10 mg	20 mL	Decahydronaphthalene	BT(500) DBT(500) 4,6-DMDBT(500)	Air	100 °C	180 min	75% 100% 100%	[88]
Cu NPs/g-BN	570	100 mg	40 mL	Decalin	DBT(500) 4,6-DMDBT(500)	Air	120 °C	480 min 180 min	99% 97%	[89]
Pt@h-BN	-	50 mg	40 mL	Decalin	BT(500) DBT(500) 4-MDBT(500) 4,6-DMDBT(500)	Air	130 °C	360 min	85.9% 98.3% 96.5% 93.7%	[51]
5-MoOxNPs/g-BN	108	100 mg	20 mL	Decalin	DBT(500) 4-MDBT(500) 4,6-DMDBT(500)	Air	120 °C	180 min 270 min 270 min	100% 97% 97%	[90]
C ₈ V/g-BN	493	80 mg	40 mL	-	DBT(500) DBT(600) DBT(800) DBT(1000) 4-MDBT(500) 4,6-DMDBT(500)	Air	120 °C	240 min 300 min 300 min 360 min 300 min 300 min	99.8% 99.6% 96.6% 95.9% 99.5% 95.3%	[91]
BN-1	-	50 mg	20 mL	Decalin	DBT(500) 4-MDBT(500) 4,6-DMDBT(500)	Air	130 °C	480 min	98.2% 97.5% 98%	[92]
V ₂ O ₅ /BNNS	-	200 mg	50 mL	-	DBT(500) 4-MDBT(500) 4,6-DMDBT(500)	Air	120 °C	240 min	99.6% 97.1% 95.2%	[93]
BCN-20	-	70 mg	20 mL	Decalin	DBT(200) 4-MDBT(200) 4,6-DMDBT(200)	Air	100 °C	360 min	100% 90.5% 98.7%	[94]
BCN-1	1004	50 mg	20 mL	Decalin	DBT(500) 4-MDBT(500) 4,6-DMDBT(500)	Air	125 °C	240 min	98.4%	[95]
TMAC-BCNO	838	50 mg	20 mL	Dodecane	DBT(200) 4-MDBT(200) 4,6-DMDBT(200)	Air	125 °C	360 min	99%	[96]
B ₄ C-5	-	50 mg	20 mL	Dodecane	DBT(200) 4-MDBT(200) 4,6-DMDBT(200)	Air	130 °C	480 min	99.5% 91% 97.5%	[97]
20% V-IL/ 3D g-C ₃ N ₄	46.99	10 mg	20 mL	Dodecane	DBT(200) 4,6-DMDBT(200)	Air	120 °C	360 min	97.2% 95.8%	[98]
Au- TiO ₂ @C ₃ N ₄ - 800	-	10 mg	20 mL	Dodecane	DBT(200) 4-MDBT(200) 4,6-DMDBT(200)	Air	120 °C	360 min	99.7% 98.8% 99.4%	[99]

5.1. Reduced Graphene Oxide (rGO)

In 2017, Gu et al. [58] chose reduced graphene oxide (rGO) as catalysts in AODS of model oils for the first time. The rGO material displayed 100% DBT removal with quite low catalyst dosage (8.7 wt%) at 140 °C in 2 h, which proved that the material was superior to many other carbon-based materials. The XPS and other control experiments indicated that the carbonyl groups, generated in situ on the chemical active defects of rGO, were efficient active sites for aerobic desulfurization of refractory sulfur compounds. The carbonyl groups facilitated the activation of oxygen by altering the electronic structures of the adjacent carbon atoms at the rGO surfaces. The reactive oxygen species was reported to be rGO-OO*⁻. This work inspired the application of carbon material into AODS process.

In the work of Ma et al. [88], monodisperse POM clusters was immobilized on graphene using poly (ionic liquid) (PIL) as linker and used as AODS catalyst. The monodis-

persed active sites, high specific surface area and large mesoporous size endowed the catalyst excellent desulfurization performance. DBT could be completely converted into DBT-sulfone at 100 °C in 3 h with an air flow of 25 mL/min. Detailed tests for desulfurization of model fuel were carried out to explore the influence of crucial parameters. Under the optimal reaction conditions, the catalyst could remain stable at least six times without noticeable decreases of the catalytic performance.

5.2. Boron-Nitride-Based Materials

Recently, graphene-like boron nitride (g-BN) had been developed new application as a catalyst for aerobic catalysis due to large surface area and high chemical stability [100]. However, its insulating properties prevented it from becoming a highly active material. In the work of Wu et al. [89], copper nanoparticles (Cu NPs) with low resistivity confined in g-BN (Cu NPs/g-BN) showed an enhanced performance than pristine g-BN in aerobic oxidation of aromatic sulfur compounds, with a sulfur removal of 98% at 120 °C in 8 h. In addition, the catalyst could be recycled for 10 times, and significantly reduction was not observed, which was attributed to the enhancement of electron mobility coming from the idiosyncratic oxidation-resisting property of Cu NPs. The existence of g-BN can protect Cu NPs from being oxidized. This strategy enlarges the application of g-BN for aerobic reactions.

Platinum group nanoparticles are one of the most attractive AODS catalysts due to their high catalytic activities. However, the high surface energy of platinum nanoparticles (Pt NPs) led to the unwanted sintering effect, deactivating the catalyst. In another work by Wu et al. [51], strong metal-edge interactions (SMEI) between Pt NPs and non-reducible hexagonal boron nitride (h-BN) support were established and made the Pt NPs well dispersed, avoiding the reversible process of classic strong metal-support interactions (SMSI) in oxygen. A DBT removal of 98.3% could be reached at 130 °C with a TOF value of 15.33 h⁻¹. The extraordinary AODS performance was attributed to the high dispersion of Pt NPs and the formation of SEMI, which facilitated the electron transfer between Pt NPs and h-BN, then improved the adsorption and activation of O₂. The sulfur removal rates of ibenzothiophene, 4, 6-dimethyldibenzothiophene, 4-methylbenzothiophene, and benzothiophene was 98.3%, 96.5%, 93.7% and 85.9%, respectively.

Yao et al. [90] anchored molybdenum oxide nanoparticles (MoO_xNPs) on g-BN by a simple one step method. The particle size of MoO_x NPs could be controlled by the amount of precursor, which removed the large particle size occurring in a routine high temperature calcination method. The controlled MoO_xNPs size integrated with strong metal oxide support interaction contributed to high aerobic oxidative desulfurization activity. A high TOF value of 37.5 h⁻¹ could be achieved at 120 °C. Moreover, 98.0% DBT sulfur removal was still achieved after recycling 11 times, as shown in Figure 10, indicating a good stability and recycling performance of supported catalyst.

A series of g-BN supported decavanadate ionic liquids (POM-IL) [91] was synthesized and exhibited remarkable AODS performance owing to the inherent catalytic ability of POM-ILs and the high surface area of g-BN. When using C₈V/g-BN as catalyst, the DBT removal could reach 99.8% (≤1 ppm) at 120 °C in 4 h with a TOF value of 42.99 h⁻¹, and it could remain stable after six cycles. On the other hand, excellent performance in oils with different sulfide substrates, concentrations and aromatics/olefins addition was also achieved. This facile method could reduce the dosage and enhance the stability of pristine POM-ILs.

Wu et al. [92] developed a facile and environment-friendly liquid nitrogen gas exfoliation method to achieve porous monolayer nanosheets (BN-1). As Figure 11 shown, compared with bulk BN, the sulfur removal of porous monolayer structure h-BN (BN-1) could reach 98.2% under the same condition, achieving deep desulfurization. With the decrease of the layer numbers, the sulfur removal increased owing to the reduction of lateral sizes and more exposed active sites. The results indicated that the more edge generation through increasing exfoliation cycles, the higher catalytic activity. Moreover, the catalyst

can be recycled eight times without significant decrease in aerobic catalytic oxidation of sulfur compounds, indicating the stability of the gas exfoliation 2D materials.

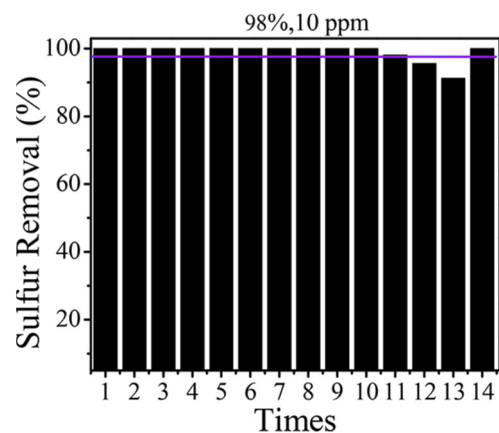


Figure 10. Recycling performance of MoOxNPs/g-BN. Reaction conditions: $V(\text{oil}) = 20 \text{ mL}$, $m(\text{catalyst}) = 0.1 \text{ g}$, $T = 120 \text{ }^\circ\text{C}$, $v(\text{air}) = 100 \text{ mL/min}$, $t = 8 \text{ h}$ [90].

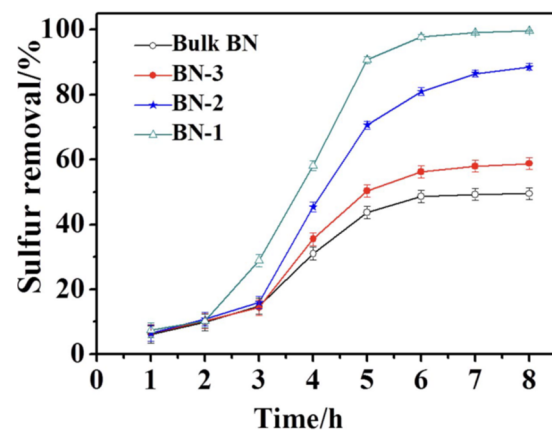


Figure 11. Effect of exfoliation cycles on sulfur removal [92].

On the basis of the gas-exfoliated BN nanosheets (BNNS), Wang et al. [93] introduced 2D V_2O_5 to the BNNS carrier and constructed a 2D-2D nanocomposites via a convenient solvothermal method. The characterization results confirmed the successful introduction of 2D V_2O_5 . The catalytic aerobic oxidation performance of the 10 wt% $\text{V}_2\text{O}_5/\text{BNNS}$ nanocomposites was much higher than that of the BN-1, which obtained deep desulfurization (DBT, $\leq 2 \text{ ppm}$) under $120 \text{ }^\circ\text{C}$ in 4 h, providing an efficient fabrication strategy to design AODS catalyst and produce ultralow S-content oils. Moreover, deep desulfurization of oils with different substrates and distractors could also be achieved. In addition, the reaction system could be recycled at least seven times without any appreciable. The exposed (0 0 1) facets of V_2O_5 , unsaturated V sites as well as oxygen vacancies contributed together to the extraordinary performance of the 2D-2D nanocomposites.

5.3. Boron Carbon Nitride (BCN)-Based Materials

That electronic properties can strongly affect the performance of h-BN catalysts was reported. Heteroatom doping was an effective way of taming electronic structure [101,102]. A carbon-doped h-BN (BCN) [94] was prepared by employing the ionic liquid (IL) as carbon source. The obtained metal-free heterogeneous catalyst BCN-x showed an outstanding catalytic performance for the AODS reaction, where a completely sulfur removal could be achieved at $100 \text{ }^\circ\text{C}$ and atmospheric pressure. The sulfur removal could still be remained 92% after 5 cycles. Furthermore, it was discovered that the doped carbon atoms bonded

with the N atoms and promoted the formation of π electrons, thus improving the electron delocalization effect of BN and facilitating the activation of molecular oxygen.

The catalytic performance of BCN was closely related to the edge electronic structures [103]. However, the carbon in BCN tended to agglomerate and form separate graphene and BN domain. Therefore, homogeneity was vital for the catalytic performance of BCN materials. In the face of this issue, Wei et al. [95] synthesized a hierarchical porous BCN catalyst using a ternary deep eutectic solvent (DES) as the template and more even precursor, as shown in Figure 12. The as-prepared BCN showed excellent catalytic AODS performance with a sulfur removal of 98.4% at 125 °C in 4 h. It can be recycled 5 times with a little activity decrease. The uniform dispersion of carbon clusters improved the electron delocalization effect of BCN. Combined with density functional theory (DFT), the improved electron delocalization would increase the electron density of BCN and promote the activation of molecular oxygen, thus reducing the reaction temperature required for the AODS process.

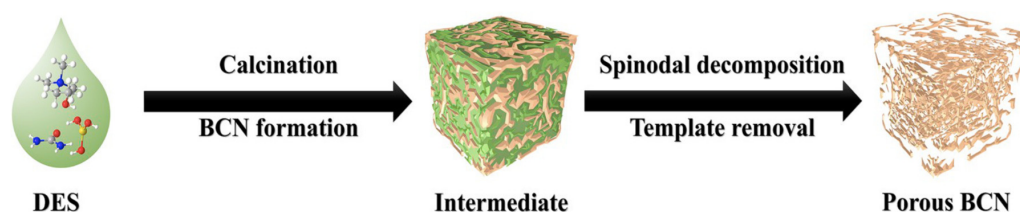


Figure 12. The synthetic route diagram of the porous BCN catalyst [95].

The heteroatom-doped h-BN catalysts can have atomic disorder at the grain boundaries. There are different configurational entropies on various atomic short-range orderings or phase separations, leading different performance for catalytic reactions. To explore the effect of configurational entropies on the AODS catalytic activity, Wei et al. [97] synthesized a series of carbon and oxygen co-doped h-BN (BCNO) catalysts with different atomic orderings using DES as precursor. The low steric resistance DES was investigated as a trend of high-entropy structures (HES) in the BCNO (high density of grain boundaries). Moreover, it was found that the HES was a booster for the radical initiation of AODS of diesel. Figure 13 showed that TMAC-BCNO with the lowest steric effect exhibited the shortest induction period and achieved complete sulfur conversion in 6 h, compared with the pure h-BN. The improvement of catalytic performance of BCNO can be attributed to the sufficient reactive sites in HES.

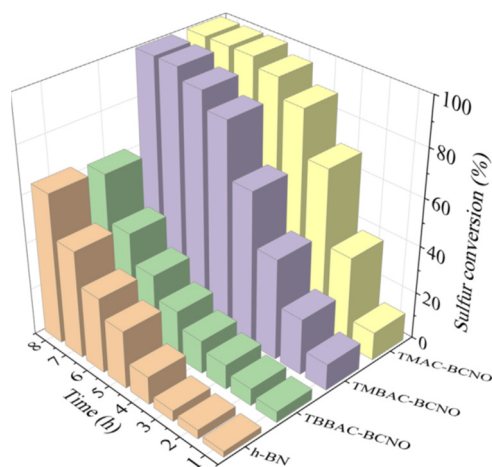


Figure 13. The results of aerobic ODS tests on DBT model diesel for the BCNO catalysts [96].

Boron carbide (B_4C) has been attracted much attention due to its extremely high thermal stability, low density and excellent high-temperature thermoelectric properties.

Therefore, it was good candidate to promote AODS reaction. Wu et al. [97] had successfully prepared a metal-free B_4C by mechanical ball milling exfoliation, which induced thinner-layered structure, small size and numerous defects in B_4C catalysts, as shown in Figure 14. It was investigated that the defects functioned as catalytically active sites. Furthermore, the exfoliated boron carbide catalyst was applied in aerobic ODS system, and sulfur removal reach 99.5% at $130\text{ }^\circ\text{C}$ in 8 h. Moreover, the catalyst could be recycled 17 times without a significant decrease in catalytic activity, indicating their inherent robustness. In particular, it was found that the current aerobic ODS system could remove 90% sulfur compounds in real diesel oil.

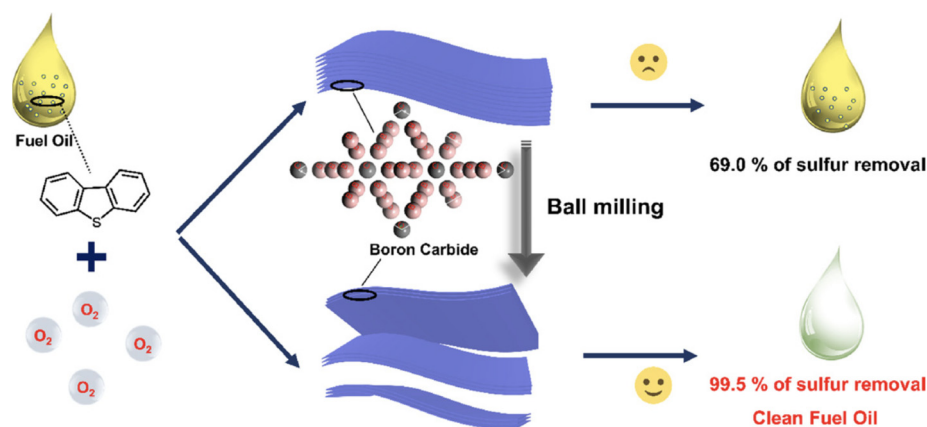


Figure 14. Scheme of exfoliated metal-free boron carbide for aerobic oxidative desulfurization [97].

5.4. Porous Carbon Nitride

In 2020, Gu et al. [98] synthesized a three-dimensional (3D) porous $g\text{-}C_3N_4$ supported vanadium-based heterogeneous catalyst (V-IL/3D $g\text{-}C_3N_4$) by a simple solvothermal method. The as-prepared $g\text{-}C_3N_4$ carrier has a rich 3D pore structure, which was beneficial to the high dispersion of active center, while the mesoporous $g\text{-}C_3N_4$ can adsorb sulfur compounds and enhance the mass transfer of reaction. The experimental results showed that small amount (0.01 g) of the catalyst can activate the oxygen in the air, and oxidize different refractory organic sulfur compounds in the model oil to polar sulfones. The catalyst could maintain stable catalytic activity in five cycles, indicating the excellent cycle stability of the catalyst.

As mentioned earlier in Section 5.2, the SMEI could facilitate the dispersion of platinum group metals with high surface energy and promote the AODS reaction [51]. However, for supported Au NPs, the interactions between metal NPs and the support are not easily constructed due to their low surface energy and low work function. To solve this problem, Liu et al. [99] developed a novel C_3N_4 -mediated synthetic strategy to fabricate an Au/ TiO_2 nanoparticles (NPs) catalyst with SMSI between the TiO_2 support and Au NPs. The C_3N_4 layer on TiO_2 functioned as a sacrificial agent, mediating the formation of a SMSI between the reducible TiO_2 support and Au NPs. Compared with the catalyst supported Au NPs without SMSI, both of the activity and stability of catalyst with SMSI was improved. The TOF value was 40.77 h^{-1} for Au- $TiO_2@C_3N_4$ -800, which was much higher than that of Au- TiO_2 -800 (28.33 h^{-1}) under the same reaction conditions. After 6 h of reaction, the catalytic activity was arranged in following rank order according to performance: DBT > 4,6-DMDBT > 4-MDBT. Moreover, sulfur removal can still remain at 92.2% after being reused seven times, indicating the excellent stability owing to the formation of a SMSI.

6. Conclusions and Prospects

The stringent limitation of petroleum refinery sulfur emission urged the removal of sulfur compounds as a critical issue. As a result, AODS had received substantial consideration in last decades. This reaction could be an ideal way to perform the ODS process

because the oxidant is abundant, available everywhere and inexpensive. On the other hand, the number of research papers related to porous materials increased significantly in recent years, concerning the reaction of oxidation with molecular oxygen in the absence of sacrificial compounds. Several breakthroughs were achieved in the development of an efficient porous material catalyst for AODS. Based on the catalyst structure and catalytic performance introduced in the current paper, the following conclusions could be drawn:

- Porous mixed metal oxides catalysts are desirable due to their tunable electronic structure, which could facilitate the activation of molecular oxygen.
- For composites of mesoporous silica and metal oxides composites, the interaction between carriers and active center, dispersion of metal oxides and the formation of metal peroxides resulting in improved activity and stability of the catalysts in AODS process.
- In MOF-based catalysts, the coordinatively unsaturated metal sites, tailorable organic linkers, high surface area joined with unique porosity endowed MOFs with both the ability to catalyze AODS themselves and to be supports for active centers.
- Porous graphene-based catalysts are promising catalysts due to their excellent mechanical stability, rich surface defects or functional groups, and high surface area.
- Boron nitride-based catalysts are the new favorite of researchers owing to their high specific surface area, extremely high thermal stability, non-reducibility and tunable electronic structure, which are desirable in both supported metal-containing catalysts and metal-free catalysts.

It is envisioned that porous materials have great potential in aerobic oxidation of organosulfur compounds. Future interest may lie in increasing exposed active sites, tunable electronic structure and stability of porous catalysts. However, the AODS temperature is still relatively too high, which will lead to the side reaction for oxidation of the petroleum components and affect the octane number of the commercial gasoline or diesel products. In the future, more attention should be devoted to designing catalysts that function at a lower temperature. Low temperature catalysis recently occurred when using catalysts with a reasonable electronic structure, which would find a more promising scenario in the field of AODS catalysis. Future work should also be focused on the synthesis and in-depth mechanism study, paving a way for the rational design of the next-generation catalysts for AODS reactions.

Author Contributions: Writing—original draft preparation, B.Y. and X.L.; writing—review and editing, B.Y. and X.L.; supervision, Y.S.; funding acquisition, X.L. and Y.S. All authors have read and agreed to the published version of the manuscript.

Funding: This research was funded by Guangdong Basic and Applied Basic Research Foundation, grant number 2019A1515110532, Guangdong Basic and Applied Basic Research Foundation grant number 2021A1515011808, Post-doctoral Foundation Project of Shenzhen Polytechnic, grant number 6021330013K0.

Data Availability Statement: The data presented in this review are available in all the references.

Conflicts of Interest: The authors declare no conflict of interest.

References

1. Martin, J.M.C.; Sanchez, M.C.C.; Presas, P.P.; Fierro, J. Oxidative processes of desulfurization of liquid fuels. *J. Chem. Technol. Biotechnol.* **2010**, *85*, 879–890. [[CrossRef](#)]
2. Srivastava, V.C. An evaluation of desulfurization technologies for sulfur removal from liquid fuels. *RSC Adv.* **2012**, *2*, 759–783. [[CrossRef](#)]
3. Abotsi, G.; Scaroni, A.W. A review of carbon-supported hydrodesulfurization catalysts. *Fuel Process. Technol.* **1989**, *22*, 107–133. [[CrossRef](#)]
4. Shafiq, I.; Shafique, S.; Akhter, P.; Yang, W.; Hussain, M. Recent developments in alumina supported hydrodesulfurization catalysts for the production of sulfur-free refinery products: A technical review. *Cat. Rev.* **2020**, *5*, 1–86. [[CrossRef](#)]
5. Ahmed, I.; Jhung, S.H. Adsorptive desulfurization and denitrogenation using metal-organic frameworks. *J. Hazard. Mater.* **2016**, *301*, 259–276. [[CrossRef](#)]

6. Yang, R.T.; Hernández-Maldonado, A.J.; Yang, F.H. Desulfurization of Transportation Fuels with Zeolites Under Ambient Conditions. *Science* **2003**, *301*, 79–81. [[CrossRef](#)]
7. Khan, N.A.; Hasan, Z.; Jhung, S.H. Ionic Liquids Supported on Metal-Organic Frameworks: Remarkable Adsorbents for Adsorptive Desulfurization. *Chem.-A Eur. J.* **2014**, *20*, 338. [[CrossRef](#)]
8. Tian, F.; Wu, W.; Jiang, Z.; Liang, C.; Yang, Y.; Ying, P.; Sun, X.; Cai, T.; Li, C. The study of thiophene adsorption onto La(III)-exchanged zeolite NaY by FT-IR spectroscopy. *J. Colloid Interface Sci.* **2006**, *301*, 395–401. [[CrossRef](#)]
9. Yu, F.; Liu, C.; Yuan, B.; Xie, P.; Xie, C.; Yu, S. Energy-efficient extractive desulfurization of gasoline by polyether-based ionic liquids. *Fuel* **2016**, *177*, 39–45. [[CrossRef](#)]
10. Asumana, C.; Yu, G.; Li, X.; Zhao, J.; Liu, G.; Chen, X. Extractive desulfurization of fuel oils with low-viscosity dicyanamide-based ionic liquids. *Green Chem.* **2010**, *12*, 2030–2037. [[CrossRef](#)]
11. Kumar, S.; Srivastava, V.C.; Nanoti, S.M. Extractive Desulfurization of Gas Oils: A Perspective Review for Use in Petroleum Refineries. *Sep. Purif. Rev.* **2017**, *46*, 319–347. [[CrossRef](#)]
12. Zhao, H.; Baker, G.A.; Wagle, D.V.; Ravula, S.; Zhang, Q. Tuning Task-Specific Ionic Liquids for the Extractive Desulfurization of Liquid Fuel. *ACS Sustain. Chem. Eng.* **2016**, *4*, 4771–4780. [[CrossRef](#)]
13. Song, C. An overview of new approaches to deep desulfurization for ultra-clean gasoline, diesel fuel and jet fuel. *Catal. Today* **2003**, *86*, 211–263. [[CrossRef](#)]
14. Desai, K.; Dharaskar, S.; Pandya, J.; Shinde, S. Ultrasound-assisted extractive/oxidative desulfurization of oil using environmentally benign trihexyl tetradecyl phosphonium chloride. *Environ. Technol. Innov.* **2021**, *24*, 101965. [[CrossRef](#)]
15. Collins, F.M.; Lucy, A.R.; Sharp, L.C. Oxidative desulphurisation of oils via hydrogen peroxide and heteropolyanion catalysis. *J. Mol. Catal. A-Chem.* **1997**, *117*, 397–403. [[CrossRef](#)]
16. Grossman, M.J.; Durrant, L.R. Biodesulfurization. In *Encyclopedia of Catalysis*; John Wiley & Sons, Inc.: Hoboken, NJ, USA, 2002.
17. Soleimani, M.; Bassi, A.; Margaritis, A. Biodesulfurization of refractory organic sulfur compounds in fossil fuels. *Biotechnol. Adv.* **2007**, *25*, 570–596. [[CrossRef](#)]
18. Gu, Y.; Ye, G.; Xu, W.; Zhou, W.; Sun, Y. Creation of Active Sites in MOF-808(Zr) by a Facile Route for Oxidative Desulfurization of Model Diesel Oil. *ChemistrySelect* **2020**, *5*, 244–251. [[CrossRef](#)]
19. Gu, Y.; Luo, H.; Xu, W.; Zhou, W.; Sun, Y. Fabrication of MOF-808(Zr) with abundant defects by cleaving ZrO bond for oxidative desulfurization of fuel oil. *J. Ind. Eng. Chem.* **2022**, *105*, 435–445. [[CrossRef](#)]
20. Ye, G.; Gu, Y.; Zhou, W.; Xu, W.; Sun, Y. Synthesis of Defect-Rich Titanium Terephthalate with the Assistance of Acetic Acid for Room-Temperature Oxidative Desulfurization of Fuel Oil. *ACS Catal.* **2020**, *10*, 2384–2394. [[CrossRef](#)]
21. Ye, G.; Hu, L.; Gu, Y.; Lancelot, C.; Rives, A.; Lamonier, C.; Nuns, N.; Marinova, M.; Xu, W.; Sun, Y. Synthesis of polyoxometalate encapsulated in UiO-66(Zr) with hierarchical porosity and double active sites for oxidation desulfurization of fuel oil at room temperature. *J. Mater. Chem. A* **2020**, *8*, 19396–19404. [[CrossRef](#)]
22. Guth, E.D.; Diaz, A.F. Method for Removing Sulfur and Nitrogen in Petroleum Oils. U.S. Patent US3847800A, 12 November 1974.
23. Attar, A.; Corcoran, W.H. Desulfurization of Organic Sulfur Compounds by Selective Oxidation. 1. Regenerable and Nonregenerable Oxygen Carriers. *Ind. Eng. Chem. Prod. Res. Dev.* **1978**, *17*, 102–109. [[CrossRef](#)]
24. Otsuki, S.; Nonaka, T.; Takashima, N.; Qian, W.; Ishihara, A.; Imai, T.; Kabe, T. Oxidative Desulfurization of Light Gas Oil and Vacuum Gas Oil by Oxidation and Solvent Extraction. *Energy Fuels* **2000**, *14*, 1232–1239. [[CrossRef](#)]
25. Liang, L.; Cheng, S.; Gao, J.; Gao, G.; He, M.Y. Deep Oxidative Desulfurization of Fuels Catalyzed by Ionic Liquid in the Presence of H₂O₂. *Energy Fuels* **2007**, *21*, 383–384. [[CrossRef](#)]
26. Hulea, V.; Fajula, F.; Bousquet, J. Mild Oxidation with H₂O₂ over Ti-Containing Molecular Sieves-A very Efficient Method for Removing Aromatic Sulfur Compounds from Fuels. *J. Catal.* **2001**, *198*, 179–186. [[CrossRef](#)]
27. Te, M.; Fairbridg, C.; Ring, Z. Oxidation reactivities of dibenzothiophenes in polyoxometalate/H₂O₂ and formic acid/H₂O₂ systems. *Appl. Catal. A-Gen.* **2001**, *219*, 267–280. [[CrossRef](#)]
28. Zhao, D.; Wang, J.; Zhou, E. Oxidative desulfurization of diesel fuel using a Brønsted acid room temperature ionic liquid in the presence of H₂O₂. *Green Chem.* **2007**, *9*, 1219–1222. [[CrossRef](#)]
29. Chica, A.; Corma, A.; Dómine, M.E. Catalytic oxidative desulfurization (ODS) of diesel fuel on a continuous fixed-bed reactor. *J. Catal.* **2006**, *242*, 299–308. [[CrossRef](#)]
30. Zhou, X.; Zhao, C.; Yang, J.; Zhang, S. Catalytic Oxidation of Dibenzothiophene Using Cyclohexanone Peroxide. *Energy Fuels* **2007**, *21*, 7–10. [[CrossRef](#)]
31. Bazyari, A.; Khodadadi, A.A.; Haghghat Mamaghani, A.; Beheshtian, J.; Thompson, L.T.; Mortazavi, Y. Microporous titania-silica nanocomposite catalyst-adsorbent for ultra-deep oxidative desulfurization. *Appl. Catal. B-Environ.* **2016**, *180*, 65–77. [[CrossRef](#)]
32. Mei, H.; Mei, B.W.; Yen, T.F. A new method for obtaining ultra-low sulfur diesel fuel via ultrasound assisted oxidative desulfurization. *Fuel* **2003**, *82*, 405–414. [[CrossRef](#)]
33. Ali, M.F.; Al-Malki, A.; El-Ali, B.; Martinie, G.; Siddiqui, M.N. Deep Desulphurization of Gasoline and Diesel Fuels Using Non-Hydrogen Consuming Techniques. *Fuel* **2006**, *85*, 1354–1363. [[CrossRef](#)]
34. Yu, G.; Lu, S.; Chen, H.; Zhu, Z. Diesel fuel desulfurization with hydrogen peroxide promoted by formic acid and catalyzed by activated carbon. *Carbon* **2005**, *43*, 2285–2294. [[CrossRef](#)]
35. Yang, L.; Jian, L.; Yuan, X.; Jian, S.; Qi, Y. One step non-hydrodesulfurization of fuel oil: Catalyzed oxidation adsorption desulfurization over HPWA-SBA-15. *J. Mol. Catal. A-Chem.* **2007**, *262*, 114–118. [[CrossRef](#)]

36. Zaykina, R.F.; Zaykin, Y.A.; Mamonova, T.B.; Nadirov, N.K. Radiation methods for demercaptanization and desulfurization of oil products. *Radiat. Phys. Chem.* **2002**, *63*, 621–624. [[CrossRef](#)]
37. Babich, I.V.; Moulijn, J.A. Science and technology of novel processes for deep desulfurization of oil refinery streams: A review. *Fuel* **2003**, *82*, 607–631. [[CrossRef](#)]
38. Lu, H.; Gao, J.; Jiang, Z.; Jing, F.; Yang, Y.; Wang, G.; Li, C. Ultra-deep desulfurization of diesel by selective oxidation with $[\text{C}_{18}\text{H}_{37}\text{N}(\text{CH}_3)_3]_4[\text{H}_2\text{NaPW}_{10}\text{O}_{36}]$ catalyst assembled in emulsion droplets. *J. Catal.* **2006**, *239*, 369–375. [[CrossRef](#)]
39. Lv, H.; Ren, W.; Liao, W.; Chen, W.; Li, Y.; Suo, Z. Aerobic oxidative desulfurization of model diesel using a B-type Anderson catalyst $[(\text{C}_{18}\text{H}_{37})_2\text{N}(\text{CH}_3)_2]_3\text{Co}(\text{OH})_6\text{Mo}_6\text{O}_{18}\cdot 3\text{H}_2\text{O}$. *Appl. Catal. B-Environ.* **2013**, *138–139*, 79–83. [[CrossRef](#)]
40. Yong, L.; Wang, Y.; Gao, L.; Chen, J.; He, M. Aerobic Oxidative Desulfurization: A Promising Approach for Sulfur Removal from Fuels. *ChemSusChem* **2010**, *1*, 302–306. [[CrossRef](#)]
41. Zhu, W.; Wang, C.; Li, H.; Wu, P. One-pot extraction combined with metal-free photochemical aerobic oxidative desulfurization in deep eutectic solvent. *Green Chem.* **2015**, *17*, 2464–2472. [[CrossRef](#)]
42. Mjalli, F.S.; Ahmed, O.U.; Al-Wahaibi, T.; Al-Wahaibi, Y.; Alnashef, I.M. Deep oxidative desulfurization of liquid fuels. *Rev. Chem. Eng.* **2014**, *30*, 337–378. [[CrossRef](#)]
43. Ismagilov, Z.; Yashnik, S.; Kerzhentsev, M.; Parmon, V.; Bourane, A.; Al-Shahrani, F.M.; Hajji, A.A.; Koseoglu, O.R. Oxidative Desulfurization of Hydrocarbon Fuels. *Catal. Rev.* **2011**, *53*, 199–255. [[CrossRef](#)]
44. Jean-Marie, B. Transition-metal complexes for liquid-phase catalytic oxidation: Some aspects of industrial reactions and of emerging technologies. *Dalton Trans.* **2003**, *17*, 3289–3302. [[CrossRef](#)]
45. Shiraiishi, Y.; Hirai, T.; Komosawa, I. Oxidative Desulfurization Process for Light Oil Using Titanium Silicate Molecular Sieve Catalysts. *J. Chem. Eng. Jpn.* **2002**, *35*, 1305–1311. [[CrossRef](#)]
46. Shafiq, I.; Hussain, M.; Shafique, S.; Akhter, P.; Ahmed, A.; Ashraf, R.S.; Ali Khan, M.; Jeon, B.; Park, Y. Systematic Assessment of Visible-Light-Driven Microspherical V_2O_5 Photocatalyst for the Removal of Hazardous Organosulfur Compounds from Diesel. *Nanomaterials* **2021**, *11*, 2908. [[CrossRef](#)]
47. Lu, H.; Zhang, Y.; Jiang, Z.; Li, C. Aerobic oxidative desulfurization of benzothiophene, dibenzothiophene and 4,6-dimethyldibenzothiophene using an Anderson-type catalyst $[(\text{C}_{18}\text{H}_{37})_2\text{N}(\text{CH}_3)_2]_5[\text{IMo}_6\text{O}_{24}]$. *Green Chem.* **2010**, *11*, 1954–1958. [[CrossRef](#)]
48. Murata, S.; Murata, K.; Kidena, K.; Nomura, M. A Novel Oxidative Desulfurization System for Diesel Fuels with Molecular Oxygen in the Presence of Cobalt Catalysts and Aldehydes. *Energy Fuels* **2004**, *18*, 116–121. [[CrossRef](#)]
49. Zeng, X.; Xiao, X.; Li, Y.; Chen, J.; Wang, H. Deep desulfurization of liquid fuels with molecular oxygen through graphene photocatalytic oxidation. *Appl. Catal. B-Environ.* **2017**, *209*, 98–109. [[CrossRef](#)]
50. Chen, B.; Wang, L.; Gao, S. Recent Advances in Aerobic Oxidation of Alcohols and Amines to Imines. *ACS Catal.* **2015**, *5*, 5851–5876. [[CrossRef](#)]
51. Wu, P.; Wu, Y.; Chen, L.; He, J.; Hua, M.; Zhu, F.; Chu, X.; Xiong, J.; He, M.; Zhu, W.; et al. Boosting aerobic oxidative desulfurization performance in fuel oil via strong metal-edge interactions between Pt and h-BN. *Chem. Eng. J.* **2020**, *380*, 122526. [[CrossRef](#)]
52. Dong, Y.; Zhang, J.; Ma, Z.; Xu, H.; Yang, H.; Yang, L.; Bai, L.; Wei, D.; Wang, W.; Chen, H. Preparation of Co-Mo-O ultrathin nanosheets with outstanding catalytic performance in aerobic oxidative desulfurization. *Chem. Commun.* **2019**, *55*, 13995–13998. [[CrossRef](#)] [[PubMed](#)]
53. Shafiq, I.; Shafique, S.; Akhter, P.; Abbas, G.; Hussain, M. Efficient catalyst development for deep aerobic photocatalytic oxidative desulfurization: Recent advances, confines, and outlooks. *Catal. Rev.* **2021**, *3*, 1–46. [[CrossRef](#)]
54. Shafiq, I.; Hussain, M.; Rashid, R.; Shafique, S.; Park, Y.K. Development of hierarchically porous LaVO_4 for efficient visible-light-driven photocatalytic desulfurization of diesel. *Chem. Eng. J.* **2021**, *420*, 130529. [[CrossRef](#)]
55. Shafiq, I.; Hussain, M.; Shafique, S.; Shafique, S.; Park, Y.K. Oxidative desulfurization of refinery diesel pool fractions using LaVO_4 photocatalyst. *J. Ind. Eng. Chem.* **2021**, *98*, 283–288. [[CrossRef](#)]
56. Gómez-Paricio, A.; Santiago-Portillo, A.; Navalón, S.; Concepción, P.; Alvaro, M.; Garcia, H. MIL-101 promotes the efficient aerobic oxidative desulfurization of dibenzothiophenes. *Green Chem.* **2016**, *18*, 508–515. [[CrossRef](#)]
57. Li, X.; Gu, Y.; Chu, H.; Ye, G.; Zhou, W.; Xu, W.; Sun, Y. MFM-300(V) as an active heterogeneous catalyst for deep desulfurization of fuel oil by aerobic oxidation. *Appl. Catal. A-Gen.* **2019**, *584*, 117152. [[CrossRef](#)]
58. Gu, Q.; Wen, G.; Ding, Y.; Wu, K.; Chen, C.; Su, D. Reduced graphene oxide: A metal-free catalyst for aerobic oxidative desulfurization. *Green Chem.* **2017**, *19*, 1175–1181. [[CrossRef](#)]
59. Wu, P.; Zhu, W.; Chao, Y.; Zhang, J.; Zhang, P.; Zhu, H.; Li, C.; Chen, Z.; Li, H.; Dai, S. A template-free solvent-mediated synthesis of high surface area boron nitride nanosheets for aerobic oxidative desulfurization. *Chem. Commun.* **2016**, *52*, 144–147. [[CrossRef](#)]
60. Feng, L.; Zhang, Y.; Lu, W.; Zhang, Y.; Li, C. Highly Efficient Photocatalytic Oxidation of Sulfur-containing Organic Compounds and Dyes on TiO_2 with Dual Cocatalysts Pt and RuO_2 . *Appl. Catal. B-Environ.* **2012**, *127*, 363–370. [[CrossRef](#)]
61. Zhou, X.; Shuang, L.; Hui, W.; Wang, X.; Liu, J. Catalytic oxygenation of dibenzothiophenes to sulfones based on Fe III porphyrin complex. *Appl. Catal. A-Gen.* **2011**, *396*, 101–106. [[CrossRef](#)]
62. Shi, Y.; Liu, G.; Zhang, B.; Zhang, X. Oxidation of refractory sulfur compounds with molecular oxygen over a Ce-Mo-O catalyst. *Green Chem.* **2016**, *18*, 5273–5279. [[CrossRef](#)]

63. Cao, Y.; Wang, H.; Ding, R.; Wang, L.; Liu, Z.; Lv, B. Highly efficient oxidative desulfurization of dibenzothiophene using Ni modified MoO₃ catalyst. *Appl. Catal. A-Gen.* **2020**, *589*, 117308. [[CrossRef](#)]
64. Hou, L.; Zhao, R.; Li, X.; Gao, X. Preparation of MoO₂/g-C₃N₄ composites with a high surface area and its application in deep desulfurization from model oil. *Appl. Surf. Sci.* **2018**, *434*, 1200–1209. [[CrossRef](#)]
65. Zhang, Q.; Zhang, J.; Yang, H.; Dong, Y.; Liu, Y.; Yang, L.; Wei, D.; Wang, W.; Bai, L.; Chen, H. Efficient aerobic oxidative desulfurization over Co-Mo-O bimetallic oxide catalysts. *Catal. Sci. Technol.* **2019**, *9*, 2915–2922. [[CrossRef](#)]
66. Song, Y.; Bai, J.; Jiang, S.; Yang, H.; Yang, L.; Wei, D.; Bai, L.; Wang, W.; Liang, Y.; Chen, H. Co-Fe-Mo mixed metal oxides derived from layered double hydroxides for deep aerobic oxidative desulfurization. *Fuel* **2021**, *306*, 121751. [[CrossRef](#)]
67. Liu, Y.; Han, L.; Zhang, J.; Yao, R.; Zhan, H.; Yang, H.; Bai, L.; Yang, L.; Wei, D.; Wang, W.; et al. Morphology-Controlled Construction and Aerobic Oxidative Desulfurization of Hierarchical Hollow Co-Ni-Mo-O Mixed Metal-Oxide Nanotubes. *Ind. Eng. Chem. Res.* **2020**, *59*, 6488–6496. [[CrossRef](#)]
68. Zhang, M.; Liao, W.; Wei, Y.; Wang, C.; Fu, Y.; Gao, Y.; Zhu, L.; Zhu, W.; Li, H. Aerobic Oxidative Desulfurization by Nanoporous Tungsten Oxide with Oxygen Defects. *ACS Appl. Nano Mater.* **2021**, *4*, 1085–1093. [[CrossRef](#)]
69. Wang, C.; Li, H.; Zhang, X.; Qiu, Y.; Zhu, Q.; Xun, S.; Yang, W.; Li, H.; Chen, Z.; Zhu, W. Atomic-Layered α -V₂O₅ Nanosheets Obtained via Fast Gas-Driven Exfoliation for Superior Aerobic Oxidative Desulfurization. *Energy Fuels* **2020**, *34*, 2612–2616. [[CrossRef](#)]
70. Yu, Z.; Lü, X.; Xun, S.; He, M.; Zhu, L.; Chen, H.; Yuan, M.; Fan, L.; Zhu, W. High-index planes T-Nb₂O₅ using self-assembly strategy for aerobic oxidative desulfurization in fuels. *Fuel* **2022**, *307*, 121877. [[CrossRef](#)]
71. Wang, C.; Chen, Z.; Yao, X.; Jiang, W.; Zhang, M.; Li, H.; Liu, H.; Zhu, W.; Li, H. One-pot extraction and aerobic oxidative desulfurization with highly dispersed V₂O₅/SBA-15 catalyst in ionic liquids. *RSC Adv.* **2017**, *7*, 39383–39390. [[CrossRef](#)]
72. Jiang, W.; Gao, X.; Dong, L.; Xiao, J.; Zhu, L.; Chen, G.; Xun, S.; Peng, C.; Zhu, W.; Li, H. Aerobic oxidative desulfurization via magnetic mesoporous silica-supported tungsten oxide catalysts. *Petrol. Sci.* **2020**, *17*, 1422–1431. [[CrossRef](#)]
73. Eseva, E.A.; Lukashov, M.O.; Cherednichenko, K.A.; Levin, I.S.; Akopyan, A.V. Heterogeneous Catalysts Containing an Anderson-Type Polyoxometalate for the Aerobic Oxidation of Sulfur-Containing Compounds. *Ind. Eng. Chem. Res.* **2021**, *60*, 14154–14165. [[CrossRef](#)]
74. Xun, S.; Jiang, W.; Guo, T.; He, M.; Ma, R.; Zhang, M.; Zhu, W.; Li, H. Magnetic mesoporous nanospheres supported phosphomolybdate-based ionic liquid for aerobic oxidative desulfurization of fuel. *J. Colloid Interface Sci.* **2019**, *534*, 239–247. [[CrossRef](#)]
75. Rajendran, A.; Cui, T.; Fan, H.; Yang, Z.; Feng, J.; Li, W. A comprehensive review on oxidative desulfurization catalysts targeting clean energy and environment. *J. Mater. Chem. A* **2020**, *8*, 2246–2285. [[CrossRef](#)]
76. Shafiq, I.; Shafique, S.; Akhter, P.; Ishaq, M.; Yang, W.; Hussain, M. Recent breakthroughs in deep aerobic oxidative desulfurization of petroleum refinery products. *J. Clean. Prod.* **2021**, *294*, 125731. [[CrossRef](#)]
77. Liu, Y.; Liu, S.; Liu, S.; Liang, D.; Li, S.; Tang, Q.; Wang, X.; Miao, J.; Shi, Z.; Zheng, Z. Facile Synthesis of a Nanocrystalline Metal-Organic Framework Impregnated with a Phosphovanadomolybdate and Its Remarkable Catalytic Performance in Ultradeep Oxidative Desulfurization. *ChemCatChem* **2013**, *5*, 3086–3091. [[CrossRef](#)]
78. Vallés-García, C.; Santiago-Portillo, A.; Álvaro, M.; Navalón, S.; García, H. MIL-101(Cr)-NO₂ as efficient catalyst for the aerobic oxidation of thiophenols and the oxidative desulfurization of dibenzothiophenes. *Appl. Catal. A-Gen.* **2020**, *590*, 117340. [[CrossRef](#)]
79. Ding, J.; Wang, R. A new green system of HPW@MOFs catalyzed desulfurization using O₂ as oxidant. *Chin. Chem. Lett.* **2016**, *27*, 655–658. [[CrossRef](#)]
80. Li, S.; Gao, R.; Zhang, R.; Zhao, J. Template method for a hybrid catalyst material POM@MOF-199 anchored on MCM-41: Highly oxidative desulfurization of DBT under molecular oxygen. *Fuel* **2016**, *184*, 18–27. [[CrossRef](#)]
81. Gao, Y.; Lv, Z.; Gao, R.; Zhang, G.; Zheng, Y.; Zhao, J. Oxidative desulfurization process of model fuel under molecular oxygen by polyoxometalate loaded in hybrid material CNTs@MOF-199 as catalyst. *J. Hazard. Mater.* **2018**, *359*, 258–265. [[CrossRef](#)] [[PubMed](#)]
82. Yu, H.; Peng, F.; Tan, J.; Hu, X.; Wang, H.; Yang, J.; Zheng, W. Selective Catalysis of the Aerobic Oxidation of Cyclohexane in the Liquid Phase by Carbon Nanotubes. *Angew. Chem. Int. Ed.* **2011**, *50*, 3978–3982. [[CrossRef](#)]
83. Yang, J.; Sun, G.; Gao, Y.; Zhao, H.; Tang, P.; Tan, J.; Lu, A.; Ma, D. Direct catalytic oxidation of benzene to phenol over metal-free graphene-based catalyst. *Energ. Environ. Sci.* **2013**, *6*, 793–798. [[CrossRef](#)]
84. Cao, Y.; Yu, H.; Tan, J.; Peng, F.; Wang, H.; Li, J.; Zheng, W.; Wong, N. Nitrogen-, phosphorous- and boron-doped carbon nanotubes as catalysts for the aerobic oxidation of cyclohexane. *Carbon* **2013**, *57*, 433–442. [[CrossRef](#)]
85. Long, J.; Xie, X.; Xu, J.; Gu, Q.; Chen, L.; Wang, X. Nitrogen-Doped Graphene Nanosheets as Metal-Free Catalysts for Aerobic Selective Oxidation of Benzylic Alcohols. *ACS Catal.* **2012**, *2*, 622–631. [[CrossRef](#)]
86. Dai, L.; Wei, Y.; Xu, X.; Wu, P.; Zhang, M.; Wang, C.; Li, H.; Zhang, Q.; Li, H.; Zhu, W. Boron and Nitride Dual vacancies on Metal-Free Oxygen Doping Boron Nitride as Initiating Sites for Deep Aerobic Oxidative Desulfurization. *ChemCatChem* **2020**, *12*, 1734–1742. [[CrossRef](#)]
87. Xiong, J.; Luo, J.; Yang, L.; Pang, J.; Zhu, W.; Li, H. Boron defect engineering in boron nitride nanosheets with improved adsorptive desulfurization performance. *J. Ind. Eng. Chem.* **2018**, *64*, 383–389. [[CrossRef](#)]
88. Ma, Z.; Zhang, J.; Zhan, H.; Xu, M.; Yang, H.; Yang, L.; Bai, L.; Chen, H.; Wei, D.; Wang, W. Immobilization of monodisperse metal-oxo-cluster on graphene for aerobic oxidative desulfurization of fuel. *Process Saf. Environ.* **2020**, *140*, 26–33. [[CrossRef](#)]

89. Wu, P.; Zhu, W.; Dai, B.; Chao, Y.; Li, C.; Li, H.; Zhang, M.; Jiang, W.; Li, H. Copper nanoparticles advance electron mobility of graphene-like boron nitride for enhanced aerobic oxidative desulfurization. *Chem. Eng. J.* **2016**, *301*, 123–131. [[CrossRef](#)]
90. Yao, X.; Wang, C.; Liu, H.; Li, H.; Wu, P.; Fan, L.; Li, H.; Zhu, W. Immobilizing Highly Catalytically Molybdenum Oxide Nanoparticles on Graphene-Analogous BN: Stable Heterogeneous Catalysts with Enhanced Aerobic Oxidative Desulfurization Performance. *Ind. Eng. Chem. Res.* **2019**, *58*, 863–871. [[CrossRef](#)]
91. Wang, C.; Chen, Z.; Yao, X.; Chao, Y.; Xun, S.; Xiong, J.; Fan, L.; Zhu, W.; Li, H. Decavanadates anchored into micropores of graphene-like boron nitride: Efficient heterogeneous catalysts for aerobic oxidative desulfurization. *Fuel* **2018**, *230*, 104–112. [[CrossRef](#)]
92. Wu, Y.; Wu, P.; Chao, Y.; He, J.; Li, H.; Lu, L.; Jiang, W.; Zhang, B.; Li, H.; Zhu, W. Gas-exfoliated porous monolayer boron nitride for enhanced aerobic oxidative desulfurization performance. *Nanotechnology* **2018**, *29*, 25604. [[CrossRef](#)] [[PubMed](#)]
93. Wang, C.; Qiu, Y.; Wu, H.; Yang, W.; Zhu, Q.; Chen, Z.; Xun, S.; Zhu, W.; Li, H. Construction of 2D-2D V₂O₅/BNNS nanocomposites for improved aerobic oxidative desulfurization performance. *Fuel* **2020**, *270*, 117498. [[CrossRef](#)]
94. Lu, L.; He, J.; Wu, P.; Chao, Y.; Li, H.; Tao, D. Taming electronic properties of boron nitride nanosheets as metal-free catalysts for aerobic oxidative desulfurization of fuels. *Green Chem.* **2018**, *20*, 4381–4568. [[CrossRef](#)]
95. Wei, Y.; Wu, P.; Luo, J.; Dai, L.; Li, H.; Zhang, M.; Chen, L.; Wang, L.; Zhu, W.; Li, H. Synthesis of hierarchical porous BCN using ternary deep eutectic solvent as precursor and template for aerobic oxidative desulfurization. *Micropor. Mesopor. Mat.* **2020**, *293*, 109788. [[CrossRef](#)]
96. Wei, Y.; Zhang, M.; Wu, P.; Luo, J.; Tao, D.; Peng, C.; Dai, L.; Wang, L.; Li, H.; Zhu, W. Deep eutectic solvent-induced high-entropy structures in boron nitride for boosted initiation of aerobic oxidative desulfurization of diesel. *Appl. Surf. Sci.* **2020**, *529*, 146980. [[CrossRef](#)]
97. Wu, P.; Jia, Q.; He, J.; Lu, L.; Chen, L.; Zhu, J.; Peng, C.; He, M.; Xiong, J.; Zhu, W.; et al. Mechanical exfoliation of boron carbide: A metal-free catalyst for aerobic oxidative desulfurization in fuel. *J. Hazard. Mater.* **2020**, *391*, 122183. [[CrossRef](#)]
98. Gu, J.; Liu, M.; Xun, S.; He, M.; Wu, L.; Zhu, L.; Wu, X.; Zhu, W.; Li, H. Lipophilic decavanadate supported by three-dimensional porous carbon nitride catalyst for aerobic oxidative desulfurization. *Mol. Catal.* **2020**, *483*, 110709. [[CrossRef](#)]
99. Liu, M.; He, J.; Wu, P.; Lu, L.; Wang, C.; Chen, L.; Hua, M.; Zhu, W.; Li, H. Carbon nitride mediated strong metal-support interactions in a Au/TiO₂ catalyst for aerobic oxidative desulfurization. *Inorg. Chem. Front.* **2020**, *7*, 1212–1219. [[CrossRef](#)]
100. Jiao, Y.; Du, A.; Zhu, Z.; Rudolph, V.; Lu, G.; Smith, S.C. A density functional theory study on CO₂ capture and activation by graphene-like boron nitride with boron vacancy. *Catal. Today* **2001**, *175*, 271–275. [[CrossRef](#)]
101. Wang, S.; Iyyamperumal, E.; Roy, A.; Xue, Y.; Yu, D.; Dai, L. Vertically Aligned BCN Nanotubes as Efficient Metal-Free Electrocatalysts for the Oxygen Reduction Reaction: A Synergetic Effect by Co-Doping with Boron and Nitrogen. *Angew. Chem. Int. Ed.* **2011**, *50*, 11756–11760. [[CrossRef](#)]
102. Goyal, R.; Sarkar, B.; Bag, A.; Lefebvre, F.; Sameer, S.; Pendem, C.; Bordoloi, A. Single-step synthesis of hierarchical B_xCN: A metal-free catalyst for low-temperature oxidative dehydrogenation of propane. *J. Mater. Chem. A.* **2016**, *4*, 18559–18569. [[CrossRef](#)]
103. Wu, P.; Yang, S.; Zhu, W.; Li, H.; Chao, Y.; Zhu, H.; Li, H.; Dai, S. Tailoring N-Terminated Defective Edges of Porous Boron Nitride for Enhanced Aerobic Catalysis. *Small* **2017**, *13*, 1701857. [[CrossRef](#)] [[PubMed](#)]